ACS APPLIED BIO MATERIALS

www.acsabm.org Article

In Vivo Chemogenetic Biocompatibility of Mercury as a Specific Hypercalcemia Actuator in Snail's Spinal Cord Cell Manipulation: An Extracellular Field Potential Biosensor

Sajedeh Karami, Mohammad Mahdi Doroodmand,* and Amir Mootabi-Alavi

Cite This: ACS Appl. Bio Mater. 2022, 5, 3649−3657 Read Online

ACCESS | Metrics & More | Article Recommendations | Supporting Information

ABSTRACT: The in vivo chemogenetic property of mercuric ions (Hg^{2+}) was investigated as a specific hypercalcemia actuator in snail's spinal cord cell manipulation by extracellular field potential biosensing analysis. For this purpose, a three-microelectrode system with working, counter, and pseudo reference electrodes was blindly implanted into the snail's spinal cord to electrically stimulate (triggering) the action potential with a staircase electrical voltage at a very low frequency level, along with measurement of the electrical current, as a detection system. Under optimum conditions, using the one-factor-at-a-time method, a wide linear range between 1.0×10^{-14} and 1.0×10^{-1} mol L^{-1} with correlation coefficients (R^2) >0.98 and a response time (t_{90}) of maximum 10.0 s were approximated. Percentages of relative standard deviation were estimated to be 3.08 (reproducibility, n = 50) and 7.31 (repeatability, n = 15). The detection limit was estimated to be sub 2.1×10^{-16} mol L^{-1} based on the $X_b^- + 3S_b$ definition. The reliability of this phenomenon was evidenced by the estimation of recovery percentages (between 95 and 107%) during spiking Hg^{2+} standard solutions. The probable mechanism behind this process could be attributed to the following: (i) the neuronal ephaptic coupling during electrical synchronization by a specific brain-triggered wave as a neuronal motor toolkit and (ii) chemical synchronization using a Hg^{2+} hypercalcemia actuator (biosensor). Linear correlation has been evidenced during interactions between Hg^{2+} and a calcium ionic channel's protein with a gram molecular weight of 66.2 ± 0.3 KCU. This process, therefore, caused an opening of the Ca^{2+} channel gates and majorly released the Ca^{2+} (hypercalcemia) that was detected as the main source of the measured electrical current. At this condition, ultratrace levels of Hg^{2+} ions not only were considered as nontoxic reagents but also had chemically regulating effects as ephaptic synchronizers to the neuron cells. This report may pave the way for using mercury ions at an ultratrace level for clinical controlling purposes during neuronal spinal cord cell manipulation.

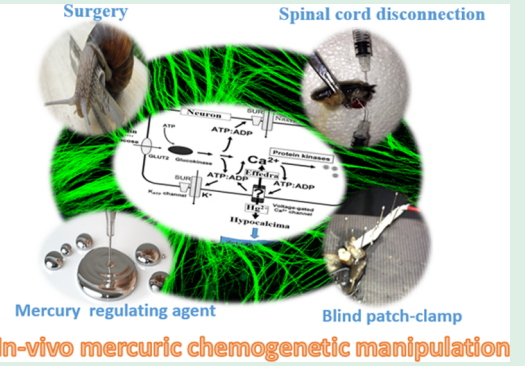

KEYWORDS: *action potential, mercury, neuromodulator, chemogenetic, snail's spinal cord cell, cell manipulation, hypercalcemia, neuron actuators*

1. INTRODUCTION

As a new scientific field, "chemogenetic" is considered among neuroscientists as a methodology in which simple molecules and elemental species interact with macromolecules.[1] This field is applicable for the efficient manipulation of different frontier systems like macromolecules (such as enzymes, hormonal, proteins, amino acids, etc.) and some living cell-type organisms (including bacteria, viruses, neuron cells, and so on).[2] It can also be noted that neuron's stimulus (triggering) both (i) electrically, using different electrical waves, and/or (ii) chemically, using chemogenetic reagents, results in cell manipulation. This process, therefore, is adopted as an efficient electrical/chemical toolkit for controlling the activity of macromolecules.[3]

Precise knowledge about the chemogenetic property (of Ca^{2+}) would therefore be important for the indirect recognition of a wide range of different neuropsychiatric symptoms, especially with regard to the neuronal cell during "malignancy-associated hypercalcemia" (MAH) infections.[4] This is because MAH infections often cause some neuronal disorders; for instance, MAH infections can cause pre-existing neurologic dysfunction, abnormality of the normal reabsorption of water medium in the renal tubule, etc.[5] In addition, MAH infections sometimes cause other diseases, such as nephrogenic diabetes insipidus with symptoms like polyuria, shortage of the glomerular filtration rate, precipitation of

Received: October 10, 2021
Accepted: January 27, 2022
Published: July 13, 2022

https://doi.org/10.1021/acsabm.1c01064
ACS Appl. Bio Mater. 2022, 5, 3649−3657

calcium phosphate salts onto the kidney tissue (i.e., nephrocalcinosis), nephrolithiasis in the presence or absence of any obstructive aeropathy, etc.[6] All of these disorders reveal the significant importance of the applied chemogenetic field for well organizing and precisely controlling hypercalcemic disorders.[7] However, to have the best result in controlling the chemotropic property, great understanding is needed about the target macromolecule and the responsible interacting species.[8]

During the last few decades, a lot of research has been reported on different chemotropic processes.[9] Most of these investigations have been limited only to various theoretical simulations at the molecular levels.[10] Although these challenges have caused some simulations, most of them have often been attributed only to simple modeling using a certain number of molecular structures or molecular fragmentations.[2] Experimental studies have almost been limited to certain biological case studies via focusing on the body-extracted proteomics or chemically when introducing some organometallic species and composites.[2] Nevertheless, many problems, especially small sensitivity and the lack of enough specificity, have restrained this scientific topic.[8]

Over the last few decades, mercury (Hg) has been considered a very harmful toxic agent, particularly for the nervous system.[11] This is because, after Hg is inhaled, it is transferred through the blood, where it is adsorbed onto the surface of nerves.[12] However, to the best of knowledge, there is no noticeable report(s) about the drugging effect(s) (biocompatibility) of this reagent and its positive influence on the nerve cells. For this purpose, in this study, for the first time, the in vivo chemogenetic property of mercuric ion (Hg^{2+}) has been investigated as a specific hypercalcemia biosensor in the snail spinal cord cell manipulation by extracellular field potential biosensing analysis. Briefly, the patch-clamp technique is a methodology with good signal quality and temporal fidelity sufficient for reporting the synaptic and ion-channel-mediated membrane potential changes, thereby enabling neurons to compute the information affected in brain disorders or by drug treatment.[13]

2. EXPERIMENTAL SECTION

2.1. Reagents and Solutions. All of the chemical reagents were analytical grade. Fresh Hg^{2+} standard solution was prepared by dissolving 0.680 ± 0.001 g of $HgCl_2{\cdot}H_2O$ (as ultrapure reference material, Merck Company, >99.99%, GMW: 271.52 g mol^{-1}) in a 250.0 mL glass volumetric flask. The ionic strength of the solution was set using a 0.01 mol L^{-1} NaCl solution (>99.0%, Merck Company). The Hg^{2+} stock reference solution was prepared using ultra-analytical grade $HgCl_2$ (as reference material, ref No: SB/FT/CS-130/2012; Merck Company, >99.9%, W/W) according to the ASTM standard (International, D6784-02). A 0.01 molar concentration ethylenedinitrilotetraacetic acid (EDTA, Merck Company) solution was also selected to stabilize the Hg^{2+} stock solution (100.0 $\mu g\ mL^{-1}$). Further stabilization of the Hg^{2+} solutions was achieved via the formation of $HgCl_4^{2-}$ using a NaCl (Merck Company) solution during the formation of Cl^- with 0.10 M concentration.

Prior to the preparation of Hg^{2+} standard solutions, the glass volumetric flasks were conditioned according to a previously reported procedure.[14] This process was achieved via sonication inside the 0.01 M acidic solution (Fluka Company) using an ultrasonic probe sonicator (Probe Sonicator, 30.0 KHz, 150.0 W, India) for 4.0 h at room temperature. For this purpose, 67.8 ± 0.1 and 12.30 ± 0.2 mg of $HgCl_2$ and NaCl reagents were, respectively, weighed and transferred into a plastic or glass volumetric flask (SG-100, 250.0 mL), followed by dilution to the mark with deionized water (DI water, a resistivity of 17.8 mΩ cm, CAS: 7732-18-5l848333-Merck Millipore). The inorganic mercury reference material (NIMS-1, Natural Inorganic Mercury Standard) was also from the Merck Company. Sequential dilutions of the stock solution were provided using deionized water. All of the Hg^{2+} standard solutions from micro- to sub-nanomolar (μM, nM) concentrations were protected under dark conditions at room temperature and diluted daily using deionized water.[14]

The effect of calcium ionic channels during the interaction between the snail neuron system and the Hg^{2+} was evaluated using two types of Ca^{2+} ionic blockers, dodecyltrimethylammonium bromide (CAS Number: 1119-94-4, Sigma-Aldrich Company) and lomerizine hydrochloride (CAS Number: 101477-54-7, Sigma-Aldrich Company).

2.2. Sub-Nanomolar Solution Preparation. Preparation of sub-nanomolar solutions with an accurate concentration is often difficult because of nonspecific adsorption and bias (significant) errors caused during multiple dilutions as the error propagation.[14] To solve this problem, according to a procedure reported in protocols,[14] four initial volumetric flasks (10.0 mL) were conditioned by filling with the interested analyte with 1.0 mmol L^{-1} concentration. These volumetric flasks were then protected at room temperature (25 °C) in a dark environment for 48.0 h. After this time period, the volumetric flasks were completely emptied out, and another fresh solution of the analyte (1.0 mmol L^{-1}) was replaced, allowing for equilibration for another 48.0 h. This process was performed at least three times, prior to emptying and conditioning the volumetric flasks for any chemical or electrochemical analysis.

To prepare the standard solutions, sequential dilutions were also made with deionized water. This process was achieved via pipetting the initial solution using an autosampler (PerkinElmer, 10.0 μL) for the preparation of standard concentrations at sub nM limits. These steps were achieved sequentially for daily dilution of the stock standard solution with mM concentration to provide different standard solutions, ranging from nano- to femtomolar (fM) limits.

2.3. Neutron Activation Analysis. Each Hg^{2+} standard solution was standardized using a prompt γ "*Neutron Activation Analysis*" (*NAA*) instrumentation (14-MeV, Ordela model 4511 N neutron detector, OPAL, Australia) based on a reference procedure.[15] For this purpose, briefly, 10.0 mL of the aqueous solution containing a fresh Hg^{2+} solution at the sub nM concentration level was introduced into the NAA system as the standard method. During the bombardment of the liquid sample with the neutrons (neutron flux: 1×10^{13} n cm^{-2} s^{-1}, kinetic energy: 2.0 keV, reaction, ^{200}Hg (n, p)^{200}Au, E_γ (MeV): 0.367−0.36, half-life: 48.0 min), the radioactive emissions (i.e., the emitted γ radiation), as well as the radioactive decay paths for each element, were detected and measured using a gas ionization detector, thereby measuring the concentration of the Hg^{2+} standard solutions.

The Hg^{2+} particles were detected with detection limits in the subparts per million range, an accuracy of less than 1.50%, a relative precision smaller than 0.10%, and an average sensitivity between $1.0 \times (10^3-10^4)$ pg Hg. The matrix of the blank solution could also be measured using related NAA reactions.[15] The NAA parameters included the following: radionuclide: ^{203}Hg, analytical mode; radiochemical neutron activation analysis, as well as irradiation, decay, and counting times (t_i, t_d, and t_c) of 20.0 h, 7.0 days, and 2.0 h, respectively, with a detector condition of the HPGe, coaxial detector, a relative efficiency of 53.0%, FWHM of 1.85 keV, and a volume of 6.0 mL in a 30.0 mL vial (1.00 cm). The measured values included the following: abundance, 0.154%; thermal cross section, 3200; resonance cross section, 472; product, ^{197}Hg; and yield, 97.0%.

2.4. Microelectrode Implant, Giga Ohm Sealed Condition, Extracellular Field Potential, Action Potential Detection, Curve Fitting, and Modulation/Demodulation Process. Microelectrode (Epoxy-Insulated Stainless Steel Microelectrode, Catalog #: 572700, A-M Systems Inc., Bedrijf) was selected for the implantation process. The microelectrode systems were implanted onto the neuron membranes by hand or using a pseudoneurotomy hand stereotaxic system (fabricated using a three-dimensional, 3-D, printer (dimension: 30 × 30 × 20 cm^3, resolution: ±0.01 mm, LulzBot TAZ 6, and a

https://doi.org/10.1021/acsabm.1c01064
ACS Appl. Bio Mater. 2022, 5, 3649−3657

stepper motor, SY42STH47-1206A), size: 42.3 mm × 48 mm, China). This process was achieved for culturing into the microchannels via adjusting the angle and position of the microelectrode system at the cerebral.

The angle and location of the microelectrode system were controlled blindly at the ganglia region of the nervous system of the gastropods based on an introduced nervous system and neural maps in the gastropod *Helix lucorum* L. system.[16] The position of the microelectrode system at an interelectrode distance of 0.25 ± 0.01 cm was also controlled blindly and randomly by implanting at different positions of the generated microfluidic channels. These channels were modified with the differentiated neuron stem cells based on only reaching the giga ohm sealed conditions in accordance with the procedure reported in our previous research.[17]

The giga ohm sealed condition was also developed based on a previously reported procedure.[18] Briefly, this was achieved via linearly (forward and backward) moving the implanted microelectrodes with hands and/or using the stepper motors, along with directly measuring the electrical resistance by a digital ohmmeter (Digital Multimeter, Fluke 115 True RMS). This giga ohm sealed condition (i.e., 6.42 ± 0.72 GΩ cm, n = 5) majorly filtered most of the external random perturbations (noises) during direct potentiometric sensing of the action potential (AP) using the implanted microelectrode system. However, for more confidence in the noise elimination process, all of the adopted components (modules) were positioned inside a cubic faraday cage (20 × 20 × 30 cm^3, stainless steel, average pore diameter: 0.2 mm) to eliminate or reduce interferences and noise.

The extracellular field potential biosensing method[19] was selected for the AP measurement when implanting a two-microelectrode system with an interelectrode distance of 0.25 ± 0.01 cm at a zero current (open-circuit) state to access the giga ohm sealed condition. The AP data were then measured using a high-resolution and high-rapid oscilloscope (RTO2000 Series Oscilloscope, up to 6.0 GHz bandwidth, R&S RT, Farnell, U.K.) inside the faraday cage. The data were then stored in the random access memory (RAM) of the oscilloscope prior to transferring them to a PC through the USB port using a written program in Visual Basic (Version 6, VB_6) software (see the Supporting Information).

The AC electrical waves at the very low frequency (VLF) region were generated using an external programmable function generator (Brand: DTC, Dulari Trading Company, Indore, Madhya Pradesh, two-channel mode, India) using the written VB_6 program. This function generator had the capability to apply a potentiostat electrical voltage at a range of ±50.00 mV (vs the total applied potential).

Voltage/current extracellular field potential biosensing (like voltammetry[19]) was adopted for applying the electrical AC stimulus using the function generator through a three-microelectrode system as working (recording), counter (auxiliary), and pseudo reference (ideally nonpolarized) microelectrodes. The ideal nonpolarization behavior of the reference microelectrode was also controlled at the outer membrane layer of the neuron ganglia. At this condition, the electrical current sampling (measuring) was also achieved using a current-to-voltage converter electronic circuit with a high-resolution and extraordinary speed operation amplifier and the "Military Series Resistance" (slew rate: <0.1 μs, OPA2626, Analog Device, China).

2.5. Snail Soma. Snail (gastropod) ganglia, due to the long neuron system network (length: 5.0 cm),[20] has often been selected as a suitable candidate for the evaluation of the AP and neuron cell research purposes. To test the AP on the neuron activity of this ganglia, several snails (year: 6.0 months, sex: male/female) were collected from a jungle area (Golestan, Iran; sampled date: June 17, 2018). After anesthetizing them with lidocaine ($C_{14}H_2N_2O$), an anesthetizing reagent (Razi Company, Iran), the snail's soma was separated (disconnected) by surgery under sterilized conditions based on a procedure reported in a protocol.[21]

The soma was protected in a suitable nutrient medium.[20] Then, the two-microelectrode system (OptiMicro Microdissection Needle Electrode, stainless steel, Type: 310; surrounded insulator: silicone; conductive tip diameter: 1.00 ± 0.01 μm; conductive height: 1.00 ± 0.01 mm; Herdsman Business Park, Osborne Park, WA 6017, Australia) was introduced into the soma with an inter-microelectrode distance of 0.25 ± 0.01 mm and a specific resistivity of maximum 6.41 ± 0.13 Ω cm. The electrical stimulation potentials were applied according to the recommended procedure, and the current results were recorded. The photographic images of the different stages of the chemogenetic process are shown in Scheme 1.

Scheme 1. Photographic Images of the Different Stages of the Chemogenetic Process

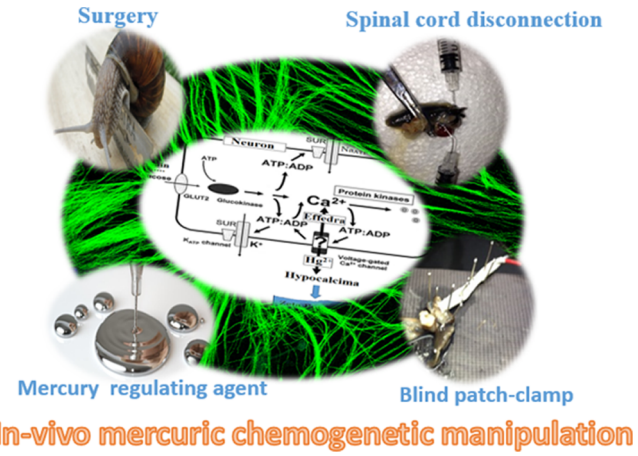

2.6. Procedure. After placing all parts of the system inside the faraday cage, the microelectrode system was implanted into the snail's spinal cord at the giga ohm sealed conditions. After that, the microelectrodes were introduced and waited for 10.0 min to gain full confidence about the wetness of the porous disks for having acceptable and tight electrical connectivity. Then, the AP was detected using the extracellular field potential with a two-electrode (indicator and pseudo reference) system with an interelectrode distance of 0.25 ± 0.01 cm at the giga ohm sealed condition. Next, a fixed potentiostat AC stimulating excitation potential signal (waveform) was applied (triggered) to the AP hyperpolarization zone through the three-microelectrode system (working, counter, and pseudo reference as the recording, auxiliary, and ideal nonpolarized microelectrode systems, respectively). Simultaneously, the electrical current was measured (sampled) by the AP voltage/current extracellular field potential methodology. The chemogenetic effect of mercuric ions (at sub nM concentrations) was evaluated via the direct injection (10.0 μL) of each solution, individually, from the position of pseudo reference electrode position (at the spinal cord membrane) using a Hamilton glass microliter syringe (50.0 μL, SETonic Microsyringes, Germany). For gaining full confidence about the reliability of the data acquisition, each datum was reported via averaging at least 10 sequential data. In addition, Q-test (degrees of freedom: 9, confidence level: 95.0%) was applied to each datum to achieve accurate and reliable data processing.

2.7. Ion Chromatography. The concentrations of each different ionic species such as Cl^-, K^+, Na^+, and Ca^{2+} ions and the interaction between Hg^{2+} and desorbed ion(s) were measured via direct sampling (20.0 μL) of the intercellular fluid from the pseudo reference microelectrode position after a fixed time scale (20.0 min) using an autosampler (LC-4000 Series, China). Each sample was then diluted 100.0 times by the deionized water and flited using a sintered glass Buchner funnel (Fisher Scientific, Fisherbrand, Fisher Scientific). Then, the cationic and anionic species were simultaneously analyzed with the ion chromatography equipment (Eco IC, 2.925.0020, Metrohm AG Company, Ionenstrasse 9100 Herisau, Switzerland) for the qualitative analysis and declaration of the probable mechanistic process according to the procedure reported in an ASTM international guideline.

As for the IC equipment, a couple of two-cationic and anionic ion-exchange resin-based column (length: 20.0 ± 0.1 cm, Waters, with

https://doi.org/10.1021/acsabm.1c01064
ACS Appl. Bio Mater. 2022, 5, 3649−3657

−COOH and $-N(O\text{-}CH_3)H_3^+$ functional groups, respectively) was adopted as the stationary phase and a Datome-filled column (5.0 cm, Shimadzu) was used as a guard column. The mobile phase included CH_3OH/H_2O (high-performance liquid chromatography, HPLC, grade 30.0%, V/V). The analytical process was achieved at 1100 ± 2 Pa pressure and 25 °C and pH buffer conditions using a phosphate buffer solution (0.01 mol L^{-1}, Merck Company). The suppressor module as a four-way alternative transmitting clocking pathways included ionic strength controlling using deionized water, pH buffer condition, mobile phase transition, and deionized water as the electrical conductivity (EC) detector's cleaner reagent.

2.8. Statistical Tests. The optimization process was based on the one-factor-at-a time method authentically using the VB_6 program during rapid and sequential data acquisition through the electronic interface and the USB port. Each sampled datum was again reported via averaging at least 10 sequential data acquisition with a time interval of 25.0 ± 0.1 μs time interval. A *t*-test method with a 95.0% confidence level and 9 degrees of freedom was evaluated for evaluation of the significance of each measured datum. The error bars were based on the ±standard deviation (n = 10). The *t*-test was also adopted for evaluation of the normal distribution of the sampled current after applying each AC stimulus waveform.

2.9. Ionic Responsible Channel(s): Selectivity to the Ca^{2+} Ionic Channel. Each Ca^{2+} containing an ionic blocker solution (20.0 μL) was introduced to the neuron system via direct injection through the pseudo reference microelectrode position at different periods of time (i.e., before and after Hg^{2+} introduction) using an autosampler.

3. RESULTS AND DISCUSSION

3.1. In Vivo Chemogenetic Effect of Mercury. Chemogenetic controlling of the electrical connectivity at the interneuron systems was considered as one of the most impotent problems in neuroscience. This challenge seemed to be more difficult when dealing with the spinal cord, at which the length of neuron cells reached even up to 1.0 m^3. In addition, electrical connectivity at the axon-dentate regions of a two-neighbor neuronal system mainly promoted this challenge.

However, from a surface point of view, this electrical connectivity obeys electrically almost from the "Classical Cable Theory"[3] as a mathematical equivalent model, but this model is able to calculate and interpret both electrical current and voltage. This model is, therefore, along the passive neurites (mainly the dendrites), which receive synaptic inputs at different sites and times.[3] As a result, this mode is originated based on the sequence of different resistance−capacitance (R−C) elements in the neuron systems. According to this model, the capacitance element of a neuronal fiber comes about as the electrostatic forces and acts through the very thin lipid bilayers. However, the appearance of the electrical resistance element in series along the fiber almost originated from the axoplasm's significant electrical resistance to the movement of electric charge.[3] These elements are related to some important factors such as the dielectric property of the neuron cells and membranes, specific resistivity of the neuronal spinal cords as well as forward rectifying behavior of some ionic channels like K^+ pumping.[3]

However, regardless of these processes, there is great demand for successive controlling of the chemogenetic behavior of the neuron systems, especially during effective treatment(s) of the large ranges of neuronal disorders. Obviously, access to these conditions needs enough knowledge about the electrical current flow through the neuronal systems. This is possible via direct electrical detection, for instance, from the cortex of the brain or optically via the detection of the electrical behavior of the neuronal systems. However, focusing on applicable methods such as "*extracellular field potential*" techniques[19] would open new horizons in the neuronal electrical systems. In the following section, this method is evaluated in detail.

3.2. Extracellular Field Potential Biosensing. In this experiment, the extracellular field potential biosensing method was utilized via implanting a two-microelectrode system into the neuron membranes by hand or using a 3-D printer (LulzBot TAZ 6) and stepper motor (SY42STH47-1206A). The selected neuron system included the differentiated stem cells[17] and/or snail's neural cords. The AP was then measured by the extracellular field potential biosensing method at the giga ohm sealed condition according to the recommended procedure.[17] However, to measure the electrical current flux, the neuron system was initially stimulated with a suitable electrical potential.[17] In this study, the results pointed to the insignificance of a wide variety of direct current (DC) potential with different electrical amplitudes, ranging between −150.0 and + 200.0 mV (vs total applied potential). However, the effect of the DC triggering process on the measured electrical current was so small that even alternative triggering of the DC waveforms with different on/off (clock) frequency domains ranging from 5 to 10 000 Hz showed a significant electrical response. Nevertheless, controlling the threshold of the triggering process on different time zones of the AP further admitted the inconsequentiality of the detected electrical current as the detection probe.

3.3. Selection of the Action Potential Triggering Voltage: Waveform Selection. In addition to the DC potential−time diagram, the effect of various types of stimulated alternative current (AC) waveforms such as normal pulse, differential pulse, square wave, cyclic voltammetry, $\sin(t)$, $\tan(t)$, and sawtooth was also evaluated in detail. This was achieved via scabbing and controlling the AC waveforms with various controlled pulse heights, pulse widths, electrical frequencies, and initial phase shifts. However, compared with those of different DC and AC waveforms, only the sawtooth signal with very low frequency showed enhancement to around 5.0% in the measured electrical currents.

3.4. Optimization. The detail of the sawtooth waveform as well as its optimization (by the one-factor-at-a time method) was evaluated in our previous study.[17] According to this report, this optimization was achieved automatically by programming the function generator by the program written with VB_6 software. The optimized responsible factors have been summarized in Figure 1. In addition, the inset of Figure 1 graphically (notations: 1−7) shows the definition of each responsible parameter related to the selected waveforms.

As shown, the peak-to-peak voltage (V_{p-p}) was defined as the voltage gradient, being high and low at a fixed wavelength. The frequency was also the period of the wave at two neighboring modes with the same phases. The pulse and relaxation time intervals were defined as the time scales at the top and bottom steps, respectively. The slope was the gradient of voltage vs time at sequential identical phasing points. As clearly shown (inset of Figure 1), the upper region of each peak (dash line) has been cut (clamped) with a fixed potential, resulting in the promotion of the sensitivity (electrical current) of the system in the absence of any clamping voltage. At this condition, the importance of this optimization was so high that around 16% enhancement was observed in the electrical current when using voltage-clamped sawtooth waveform, compared to other types of neurons triggering potentials

https://doi.org/10.1021/acsabm.1c01064
ACS Appl. Bio Mater. 2022, 5, 3649−3657

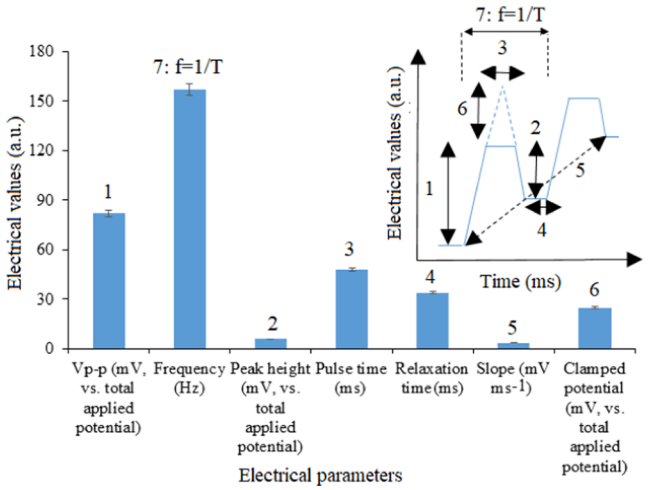

Figure 1. Optimum values of the electrical VLF signals related to the AP perturbations optimized by the one-factor-at-a-time method using VB_6 software with the voltage/current extracellular field potential system using the three-electrode system. Conditions: data are the average of three independent analyses. Error bar: ± standard deviation. Inset: Graphical (notations: 1−7) definition of each responsible parameter on the selected waveforms.

such as sin(t), square wave, normal/differential pulses, etc. This result, therefore, pointed to the effective role of the sawtooth waveform in the sensitivity of this biosystem.

3.5. Specificity of the Hyperpolarization Zone of the Action Potential to the Electric Stimulus. Further analyses on the voltage/current extracellular field potential biosensing process on the AP of the snail spinal cord revealed that the electrical response was detected only when this electrical waveform was applied at the time interval of the hyperpolarization zone of the AP (Figure 2). This was in good agreement with the results obtained on sheep's spinal cord and differentiated stem cells based on our previous research.[17]

3.6. Figures of Merit. *3.6.1. Reproducible Reducing Effect of Ultratrace Levels of Hg^{2+} Using the Voltage/Current Extracellular Field Potential Biosensing Method.* To further analyze the effects of Hg^{2+} on the electrical communication by the "Ephaptic Coupling" process between the neuron cells in the snail spinal cord, influences of some organic/inorganic species were evaluated. This was achieved via focusing on the electrical communication after stimulating the neuron by the AC stimulation. In this experiment, the control systems (cases) included the neuron cell, operated (i) in the absence of any AC electrical stimulation wave, (ii) at different AP zones, except for the hyperpolarization zone, (iii) with high-frequency AC waves, (iv) with unsuitable waveforms, (v) during demodulation of the AP after triggering with the AC waveform, and/or (vi) in the absence of any Hg^{2+} solution injection. According to the results, compared with that observed in the controls, sensitive reducing effects were observed in the electrical currents (Figure 3) during the

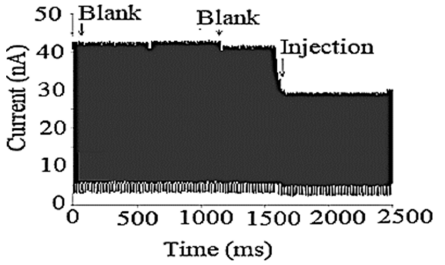

Figure 3. In vivo extracellular field potential biosensing based on the effective influence of the 1.0×10^{-10} mol L^{-1} Hg^{2+} using the voltage/current extracellular field potential biosensing method on the spinal cord. Injection volume: 1.0 μL using the three-microelectrode system implanted into the snail's spinal cord. The data are the average of five sequential data.

introduction of a Hg^{2+} solution at sub nM concentrations inside the neuron-differentiated stem cells using the voltage/current extracellular field potential biosensing method.

3.6.2. Selectivity of the Biosensor for Mercury Detection. The selectivity of this biosensor for mercury detection and recognition was also evaluated in detail. According to the results, sensitive (less than 5.0% reduction in the presence of at least 10^4-fold excess of each tested foreign species), reproducible (Figure 4A), and selective (Figure 4B) signals

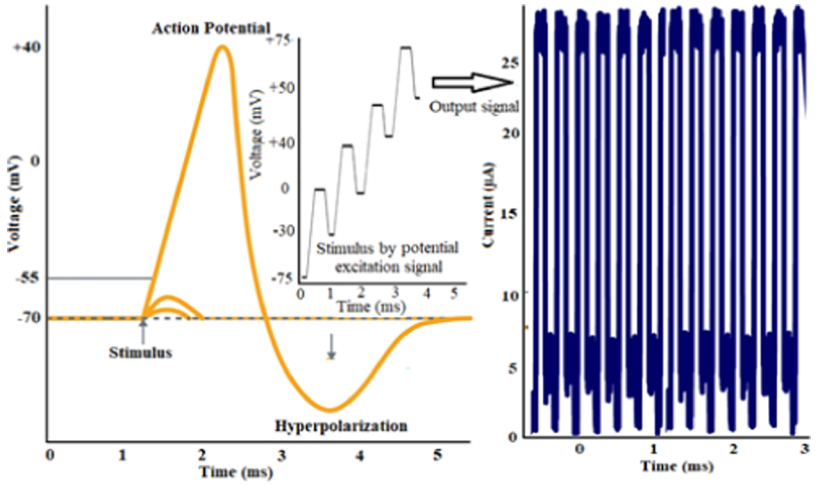

Figure 2. Specificity of the hyperpolarization zone on the neuron sensitivity. (Left) AP−time diagram. Inset: sawtooth waveform, triggered at the time scale of the hyperpolarization zone of the AP, and (right) electrical current−time curve and (inset) the optimized waveform. The data are the average of five sequential data.

https://doi.org/10.1021/acsabm.1c01064
ACS Appl. Bio Mater. 2022, 5, 3649−3657

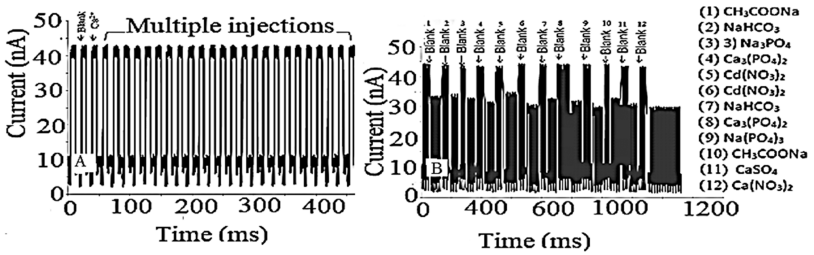

Figure 4. Electrical current−time diagrams (traces) showing (A) reproducibility and (B) selectivity in the presence of different inorganic salts as foreign reagents with 10^4-fold excess such as CH_3COONa, $NaHCO_3$, Na_3PO_4, $Ca_3(PO_4)_2$, $Cd(NO_3)_2$, $Cd(NO_3)_2$, $NaHCO_3$, $Ca_3(PO_4)_2$, $Na(PO_4)_3$, CH_3COONa, $CaSO_4$, and $Ca(NO_3)_2$ vs Hg^{2+} with 1.0×10^{-10} mol L^{-1} concentration. Injection volume: 1.0 μL using the three-microelectrode system implanted into the snail spinal cord. The data are the average of five sequential data.

were observed when directly injecting Hg^{2+} with 1.0×10^{-10} mol L^{-1} to the snail spinal cord (1.0 μL).

3.6.3. Specificity of the Stimulus Potential. As also explained previously in Figure 2, the electrical frequency of the measured current, relative to the time domain, was strongly dependent on the time duration and harmony (waveform) of the applied stimulus wave onto the AP hyperpolarization zone, whose electrical frequency can be controlled electrically. This phenomenon was also attributed to the special triggering behavior of the sawtooth waveform, compared to other types of AC-triggering systems under similar conditions (Figure 5), based on the introduced mechanistic behavior of the stimulated waveform.[17]

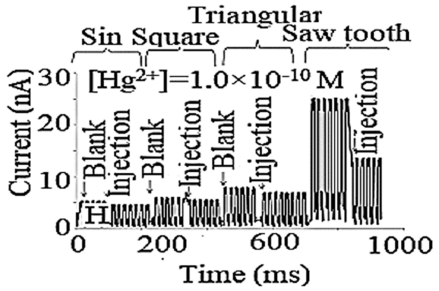

Figure 5. In vivo extracellular field potential biosensing method showing the special triggering behavior of the sawtooth waveform. Injection volume: 1.0 μL using the three-microelectrode system implanted into the snail's spinal cord. The data are the average of five sequential data.

3.6.4. Linear Range, Reproducibility, and Detection Limit of the Mercury-Based Biosensor. The linear reducing effect of the Hg^{2+} at different concentrations is also shown in Figure 6. Sequential reductions with a negative slope were detected in the electrical current with acceptable reproducibility and enough sensitivity. However, it should be noted that the injection of Hg^{2+} with higher than nM concentrations resulted in rapid death and irreversible denaturation of the snail's spinal cord and caused a significant interruption in the electrical signals under similar conditions. These results, therefore, pointed to the significance of mercury in controlling the electrical current of the spinal cord in different neuron systems.

Under optimum conditions, using the one-factor-at-a-time method, a wide linear range between 1.0×10^{-14} and 1.0×10^{-1} mol L^{-1} with correlation coefficients (R^2) >0.98 and a response time (t_{90}) of maximum 10.0 s were approximated. The percentages of relative standard deviation were estimated to be 3.08 (reproducibility, n = 50) and 7.31 (repeatability, n = 15). The detection limit was estimated to be sub 2.1×10^{-16} mol L^{-1} based on the $X_b^- + 3S_b$ definition. The reliability of this phenomenon was evidenced by different analytical techniques.

Based on the results, all of these analyses revealed the reduced electrical behavior of the neuron system vs Hg^{2+} at sub nM concentrations. This has been fundamentally in contrast to all of the previously published reports (to the best of knowledge) that introduced Hg^{2+} as a severe toxic species during the last 2 decades.[11] Thus, at this concentration, a positive drugging behavior of the Hg^{2+} is evidenced.

3.6.5. Reliability of the Mercury-Based Biosensor. The reliability of this system was evaluated via directly spiking different amounts of Hg^{2+} at sub nM concentrations and blank solution sequentially and estimation evaluation of the recovery percentages. These values were estimated to be between 95 and a maximum of 107%, suggesting the accuracy and reliability of the introduced biosensor for Hg^{2+} detection purpose, specifically, at a very short time scale.

3.7. Proposed Mechanism. The proposed mechanistic behavior of the voltage stimulus on the neuron's electrical

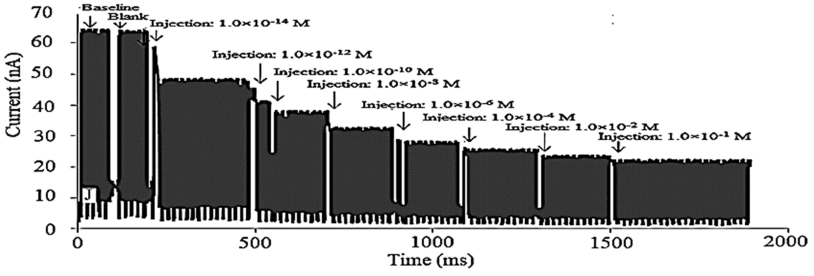

Figure 6. In vivo extracellular field potential biosensing method showing the effect of different concentrations of Hg^{2+} standard solution ranging between 1.0×10^{-14} and 1.0×10^{-1} mol L^{-1}. Injection volume: 1.0 μL using the three-microelectrode system implanted into the snail spinal cord. The data are the average of five sequential data.

https://doi.org/10.1021/acsabm.1c01064
ACS Appl. Bio Mater. 2022, 5, 3649−3657

sensitivity was investigated in detail in our previous study.[17] This process was briefly attributed to (i) "electrical" synchronization of the neuron soma (Ganglia) by this introduced specific brain-triggered electrical wave as neuronal motor toolkit; and (ii) in this study, it is further shown that this wave is regularly synchronized "chemically" by Hg^{2+} as hypercalcemia biosensors (actuators). For instance, as shown according to the electrical current−time (trace) diagram in Figure 2, as soon as the hyperpolarization zone of the AP was triggered (stimulated) electrically by the selected waveform, or chemically by these reagents, a controllable enhancement/reduction was observed in the electrical current sensitivity.

The approved pseudo quadrupole resonance between the AP hyperpolarization zone and the well-defined waveform,[17] therefore, sensitized the electrical current intensity at a steady state. This process consequently led to access-stabilized and reproducible conditions. The data acquisition process was hence continued until switching off the triggering process, at which a free induced decay was observed in the electrical current vs time until reaching the normal (untriggered and original) case. This process, therefore, revealed that the electrical frequency of the electrical current was dependent on the time duration of the applied AP stimulus waveform as the optimum electrical operator. However, this operator can further manage this system chemically. Consequently, this condition was suggested as the detection system for the chemogenetic investigation of Hg^{2+} as a suitable neuron-regulating species.

However, the specific detection of Hg^{2+} at different molar ranges, from mM to sub nM levels, is not only applicable for Hg^{2+} detection and determination inside water, air, and food sample media but also appropriate for the evaluation of the quality of any form of the inter/interim cellular media. A detailed study about this intrinsic phenomenon has been performed in vivo following the ζ-potentiometric analysis of an indicator electrode system. In this study, the differentiated stem cells were made of the sheep's spinal cord, as the ionophore, during the hypercalcemia mechanism in the presence of a Hg^{2+} solution at sub-nanomolar levels.[22] Based on this research, a linear correlation has been evidenced during the interaction between Hg^{2+} and a calcium ionic channel's protein with a gram molecular weight of 66.2 ± 0.3 KCU. This process, therefore, caused the selective opening of the Ca^{2+} channel gates and subsequently released the Ca^{2+} (hypercalcemia) that was detected as the ζ-based potentiometric response on the electrode surface.

Another main aim of this study, for the first time, is the positive effect of Hg^{2+} on the reduction of the neural abnormality of the neural electrical flow. Consequently, sub nM concentration of the Hg^{2+} solution not only has no toxicity but also exhibits a significant regulating effect on the electrical current flow by the ephaptic coupling of the neuron cell. The fabricated biosensor is, therefore, considered a simple, available, low cost, and reliable Hg^{2+} recognition probe for the potentiometric approach even for the single Hg^{2+} ion recognition.

In conclusion, this surprising phenomenon results in sensitive and fast simulation of the neuron cells. This result would therefore provide the condition for efficient treatment of neuron-based disorders according to the smart microprocessor trafficking toolkit, introduced before,[23] in addition to the promotion of the sensitivity (current intensity) of the neuron electrical transitions.

3.7.1. Responsibility of the Ca^{2+} Ionic Pumping Channel. To detect the effect of ionic channels on the electrical resistivity of the neuron system during the introduction of Hg^{2+} solutions, two different types of Ca^{2+} ionic pumping blockers (dodecyltrimethylammonium bromide and lomerizine hydrochloride) were individually introduced into the snail's spinal cord before and after Hg^{2+} introductions (Figure 7).

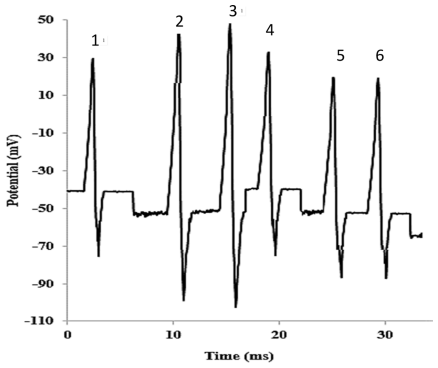

Figure 7. In vivo potential−time diagram showing the injecting effect (1.0 μL) of Ca^{2+} ionic pumping blockers (dodecyltrimethylammonium bromide and lomerizine hydrochloride) on the performance of Hg^{2+} (1.0×10^{-10} mol L^{-1}) solutions using a two-microelectrode system as the indicator and pseudo reference electrodes at open-circuit (zero current, giga ohm sealed) conditions. AP includes (1) control (in the absence of any Hg^{2+} any Ca^{2+} ionic pumping blockers), (2) and (3) demodulation of the AP potential, (4) Hg^{2+} (1.0×10^{-10} mol L^{-1}) injection, (5) and (6) sequential Hg^{2+} injection and the demodulating process after introducing Ca^{2+} ionic pumping blockers. Sample volume: 1.0 μL, using the three-microelectrode system implanted into the snail's spinal cord. The data are the average of five sequential data. Conditions: The results were evaluated after introducing Hg^{2+} (1.0×10^{-10} mol L^{-1}, 1.0 μL).

As shown in Figure 7, blocking snail's neuron cells with the Ca^{2+} blocker majorly inactivated the influence of Hg^{2+} According to this evidence, Hg^{2+} was considered as the chemogenetic actuator during interactions with the Ca^{2+} pump that resulted in having hypercalcemia conditions.

To further interpret the responsibility of the Ca^{2+} ionic channel at the sub nM concentration levels, elemental analysis was also done quantitatively using ion chromatography (IC, Figure 8) by the recommended procedure during each neuron fluidic medium sampling and the IC analysis.

Based on the chromatograms (Figure 8), no significant change was observed in the peak area of Na^+ and K^+ at

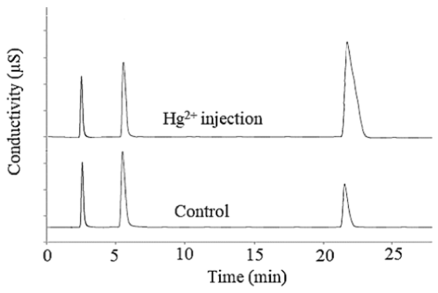

Figure 8. Ion chromatogram showing the effect of hypercalcemia biosensing process during the introduction of Hg^{2+} (1.0×10^{-10} mol L^{-1}) injected into the snail's spinal cord. Injection volume: 1.0 μL; sampled volume: 5.0 μL; dilution factor: 100 using deionized water.

https://doi.org/10.1021/acsabm.1c01064
ACS Appl. Bio Mater. 2022, 5, 3649−3657

Scheme 2. Recommended Mechanism During the Interaction Between the Snail's Spinal Cord and Hg^{2+} During the Hypercalcemia Biosensing Process

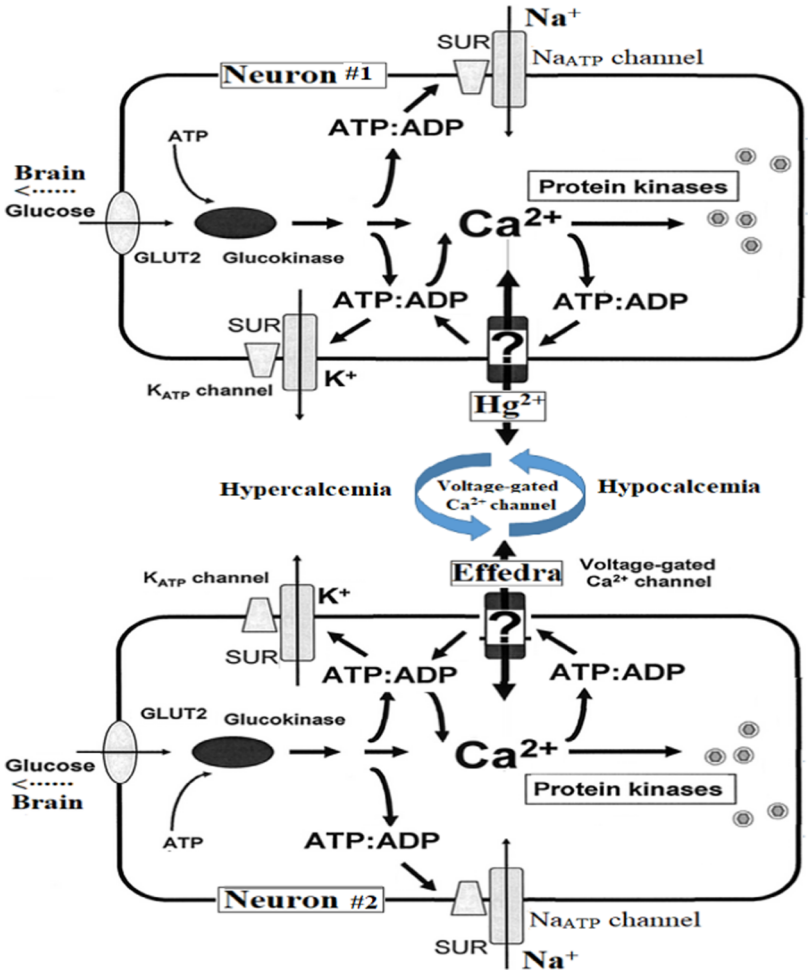

retention times of 2.52 and 5.23 min, respectively, by adopting a cationic-based resin as the stationary phase. However, a significant change was detected in the peak area of Ca^{2+} at 22.71 min retention time during sequential Hg^{2+} injections. In addition, no major change was observed in the concentration gradient of anionic species such as Cl^- under similar conditions (when using an anionic-based resin as the stationary phase). The results, therefore, revealed the direct correlation between the Hg^{2+} and Ca^{2+} release from the spinal cord tissue. Consequently, in addition to the Ca^{2+}-ionic blockers (i.e., dodecyltrimethylammonium bromide and lomerizine hydrochloride), the IC analysis confirmed the importance of Ca^{2+} ion pumping when triggering (actuating) the Ca^{2+} ionic channel gate. At this condition, therefore, Hg^{2+} is interacted, causing a Ca^{2+} influx (hypercalcemia) process. However, a reverse correlation was observed when introducing Hg^{2+}. In conclusion, the chemogenetic biocompatibility of Hg^{2+} solutions is again approved. All these pieces of evidence majorly revealed the specific neuron cell manipulation by the Hg^{2+} solutions (at the mentioned concentration levels). According to the reported information, the recommended mechanism has been graphically proposed in Scheme 2. As the final deduction, all of these consequences evidently exhibit the chemogenetic behavior of Hg^{2+} at an ultratrace level during the regulation of the electrical behavior of the neuronal systems.

Based on these results, mercury, due to its strong interaction with the neuron cells, has strong positive chemogenetic properties in the neuronal systems. This property has been mostly attributed to the controllable soft−soft interaction between mercury and different organic/inorganic-based functional groups such as C═O, C−N, etc. (such as those presented in the protein's structure), presented in the neuron tissues (see Section 3.7). It seems that the change in the spherical orientation of the protein during specific coordination with mercury causes the opening of the Ca^{2+} channel's gates, and as a result, Ca^{2+} influx from the neuron soma toward the intercellular medium. As for this intrinsic actuator, the universal behavior of this system (i.e., the selected microelectrode system) was therefore evidenced via observation of the same behavior at both in vivo and in vitro levels during the analysis of each snail spinal cord and the differentiated stem cells.[17]

4. CONCLUSIONS

The present research introduced an in vivo chemogenetic property of Hg^{2+} that was investigated as a specific hypercalcemia biosensor in snail's spinal cord cell manipulation by extracellular field potential biosensing analysis. At this condition, ultratrace levels of Hg^{2+} not only were considered as nontoxic reagents but also had regulating (positive) effects as ephaptic synchronizers to the neuron cells. Finally, this

https://doi.org/10.1021/acsabm.1c01064
ACS Appl. Bio Mater. 2022, 5, 3649−3657

report may pave the way for using mercury ions at an ultratrace level for clinical controlling purposes during neuronal spinal cord cell manipulation.

■ ASSOCIATED CONTENT

Supporting Information

The Supporting Information is available free of charge at https://pubs.acs.org/doi/10.1021/acsabm.1c01064.

Visual Basic File (FRM)

■ AUTHOR INFORMATION

Corresponding Author

Mohammad Mahdi Doroodmand − *Department of Chemistry, Shiraz University, Shiraz 71454, Iran;* orcid.org/0000-0002-6142-8540; Phone: +98-71-36137152; Email: doroodmand@shirazu.ac.ir, doroodmand@yahoo.com; Fax: +98-71-36460788

Authors

Sajedeh Karami − *Department of Chemistry, Shiraz University, Shiraz 71454, Iran*

Amir Mootabi-Alavi − *Physiological Division of Department of Basic Science, School of Veterinary Medicine, Shiraz University, Shiraz 71454, Iran*

Complete contact information is available at: https://pubs.acs.org/10.1021/acsabm.1c01064

Author Contributions

M.M.D. directed the research group, supported the necessary methods, and edited the manuscript. S.K. performed all of the chemical and biological experiments, analyzed the data, and wrote the manuscript. A.M.-A. carried out most of the biological experiments.

Funding

This study was financially supported by Shiraz University (Grant Number 135 164714).

Notes

The authors declare no competing financial interest.

Animal handling was done according to the Ethics Committee for "Animal Experiments at Shiraz University" (71454).

■ ACKNOWLEDGMENTS

The authors acknowledge the support of this work by the Shiraz University Research Council.

■ REFERENCES

(1) Atasoy, D.; Sternson, S. M. Chemogenetic Tools for Causal Cellular and Neuronal Biology. *Physiol. Rev.* **2018**, *98*, 391−418.

(2) Farrants, H.; Tarnawski, M.; Müller, T. G.; Otsuka, S.; Hiblot, J.; Koch, B.; Kueblbeck, M.; Kräusslich, H.-G.; Ellenberg, J.; Johnsson, K. Chemogenetic Control of Nanobodies. *Nat. Methods* **2020**, *17*, 279−282.

(3) Keifer, O.; Kambara, K.; Lau, A.; Makinson, S.; Bertrand, D. Chemogenetics a Robust Approach to Pharmacology and Gene Therapy. *Biochem. Pharmacol.* **2020**, *175*, No. 113889.

(4) Mirrakhimov, A. E. Hypercalcemia of Malignancy: An Update on Pathogenesis and Management. *North Am. J. Med. Sci.* **2015**, *7*, 483.

(5) Carroll, R.; Matfin, G. Endocrine and Metabolic Emergencies: Hypercalcaemia. *Ther. Adv. Endocrinol. Metab.* **2010**, *1*, 225−234.

(6) Khositseth, S.; Charngkaew, K.; Boonkrai, C.; Somparn, P.; Uawithya, P.; Chomanee, N.; Payne, D. M.; Fenton, R. A.; Pisitkun, T. Hypercalcemia Induces Targeted Autophagic Degradation of Aquaporin-2 at the Onset of Nephrogenic Diabetes Insipidus. *Kidney Int.* **2017**, *91*, 1070−1087.

(7) Konno, A.; Sukegawa, A.; Kusano, M.; Kariya, K.; Ishida, T.; Okada, H. Immunohistochemistry for Parathyroid Hormone-Related Protein (PTHrP) in Benign and Malignant Mammary Mixed Tumors of Dogs with and without Hypercalcemia. *Jpn. J. Vet. Res.* **2000**, *47*, 155−162.

(8) Galvan, A.; Caiola, M. J.; Albaugh, D. L. Advances in Optogenetic and Chemogenetic Methods to Study Brain Circuits in Non-Human Primates. *J. Neural Transm.* **2018**, *125*, 547−563.

(9) de Castro, F. Chemotropic Molecules: Guides for Axonal Pathfinding and Cell Migration during CNS Development. *Physiology* **2003**, *18*, 130−136.

(10) Grinius, L. *Energy Transduction and Gene Transfer in Chemotrophic Bacteria: Macromolecules on the Move*; Taylor & Francis, 1987; Vol. *6*.

(11) Azevedo, B. F.; Barros Furieri, L.; Peçanha, F. M.; Wiggers, G. A.; Frizera Vassallo, P.; Ronacher Simões, M.; Fiorim, J.; Rossi de Batista, P.; Fioresi, M.; Rossoni, L. Toxic Effects of Mercury on the Cardiovascular and Central Nervous Systems. *J. Biomed. Biotechnol.* **2012**, *2012*, No. 949048.

(12) Clarkson, T. W. Metal Toxicity in the Central Nervous System. *Environ. Health Perspect.* **1987**, *75*, 59−64.

(13) Jurkat-Rott, K.; Lehmann-Horn, F. The Patch Clamp Technique in Ion Channel Research. *Curr. Pharm. Biotechnol.* **2004**, *5*, 387−395.

(14) Zhang, Y.; Zeng, G. M.; Tang, L.; Chen, J.; Zhu, Y.; He, X. X.; He, Y. Electrochemical Sensor Based on Electrodeposited Graphene-Au Modified Electrode and NanoAu Carrier Amplified Signal Strategy for Attomolar Mercury Detection. *Anal. Chem.* **2015**, *87*, 989−996.

(15) Vasconcellos, M. B. A.; Catharino, M. G. M.; Paletti, G.; Saiki, M.; Bode, P.; Favaro, D. I. T.; Baruzzi, R.; Rodrigues, D. A. Determination of Mercury and Selenium in Biological Samples by Neutron Activation Analysis. *J. Trace Microprobe Tech.* **2002**, *20*, 527−538.

(16) Ierusalimsky, V. N.; Zakharov, I. S.; Palikhova, T. A.; Balaban, P. M. Nervous System and Neural Maps in Gastropod Helix Lucorum L. *Neurosci. Behav. Physiol.* **1994**, *24*, 13−22.

(17) Karami, S.; Doroodmand, M. M.; Taherianfar, M.; Mutabi-Alavi, A.; Nagshgar, N. Mechanism behind the Neuronal Ephaptic Coupling during Synchronizing by Specific Brain-Triggered Wave as Neuronal Motor Toolkit. *Sci. Rep.* **2021**, *11*, No. 3683.

(18) Braeken, D.; Prodanov, D. New Trends and Challenges in the Development of Microfabricated Probes for Recording and Stimulating of Excitable Cells. In *New Developments in Biomedical Engineering*; IntechOpen, 2010; p 311.

(19) Polder, H. R.; Weskamp, M.; Linz, K.; Meyer, R. Voltage-Clamp and Patch-Clamp Techniques. In *Practical Methods in Cardiovascular Research*; Springer, 2005; Vol. *52*, pp 272−323.

(20) Dyakonova, V.; Hernádi, L.; Ito, E.; Dyakonova, T.; Zakharov, I.; Sakharov, D. The Activity of Isolated Snail Neurons Controlling Locomotion Is Affected by Glucose. *Biophysics* **2015**, *11*, 55−60.

(21) Benjamin, P. R.; Elliott, C. J. H.; Ferguson, G. P. Neural Network Analysis in the Snail Brain. In *Model Neural Networks and Behavior*; Springer, 1985; Vol. *75*, pp 87−108.

(22) Karami, S.; Doroodmand, M. M. Chemogenetic Biocompatibly of Mercury as Specific Hypercalcemia Actuator in Neuronal Spinal Cord Cell Manipulation: Zeta Bio-Sensing Analysis. *Biosens. Bioelectron.* **2021**, *182*, No. 113125.

(23) Hassan, A. U.; Hassan, G.; Rasool, Z. Role of Stem Cells in Treatment of Neurological Disorder. *Int. J. Health Sci.* **2009**, *3*, 227.